Novel Highly Efficient In-Band Pump Wavelengths for Medium Slope Efficiency Holmium-Doped Fiber Amplifiers

Robert E. Tench, *Senior Member, IEEE*, Wiktor Walasik, and Jean-Marc Delavaux, *Senior Member, IEEE*

Abstract— **We report the design and performance of medium slope efficiency (64%) Holmium-doped fiber amplifiers (HDFAs) with novel alternative in-band pump wavelengths in the 1720–2000 nm spectral region. We demonstrate through simulations that pump wavelengths of 1840–1860 nm can yield significantly improved output power, gain, and optical-optical conversion efficiency compared to the previous technical and industry standard pump wavelength of 1940 nm. Our simulations are verified by experimental data.**

Index Terms— **Doped Fiber Amplifiers, Infrared Fiber Optics, Optical Fiber Devices, Holmium, Thulium, Polarization Maintaining Fiber, 2 microns.**

I. INTRODUCTION

Recent development of Ho-doped optical fiber amplifiers in the 2000 nm spectral region is important for many emerging applications including LIDAR, optical telecommunications, coherent lightwave systems, and spectral sensing [1]–[7]. We have previously shown that hybrid polarization maintaining (PM) Holmium-doped fiber amplifier (HDFA) architectures exhibit low noise figure (NF), high output powers, and a large operating spectral bandwidth [8]–[13]. In all these amplifiers, the HDFA is pumped at an in-band wavelength of 1940 nm which is based on a survey of the previous literature [14]–[20], [29] and also on previous technical results.

In this paper, we investigate the design and performance of medium slope efficiency HDFAs with novel alternative in-band pumping wavelengths in the 1720–2000 nm spectral region. We study in detail the performance of these amplifiers as a function of pump wavelength, pump power, signal wavelength, and signal power with both co- and counter-pumping. The results of our studies show conclusively that new pumping wavelengths in the 1720–2000 nm band yield superior results for gain, output power, and optical-optical conversion efficiency in comparison to the previously selected "standard" pump wavelength of 1940 nm which up until now has been an industry norm. The clear improvements in performance with the new or alternative pump wavelengths open the possibility of novel amplifier designs and architectures which yield much better optical-to-optical power

conversion efficiencies, considerably higher saturated output powers, and strongly enhanced small signal gains, among other benefits.

The structure of our paper is as follows: In Section II we present simulation studies for a single stage co- and counter-pumped medium slope efficiency HDFA with pump wavelengths from 1720–2000 nm. Section III covers the experimental verification of our simulations at pump wavelengths of 1860 and 1940 nm, and design directions for optimized multistage amplifiers. Finally, Section IV discusses the results of our investigations and compares our new amplifier designs to previous results from the literature.

II. SIMULATIONS OF SINGLE STAGE HDFAS WITH ALTERNATIVE PUMP WAVELENGTHS

We start our analysis by noting that in our research on HDFAs to date, we have chosen an in-band pump wavelength of 1940 nm based on a survey of the previous literature [14]–[20], [29] and also on consideration of the gain and absorption curves for the iXblue single clad Ho-doped fiber IXF-HDF-PM-8-125 [8], [14]. Figure 1 is a plot of these gain and absorption curves, where we see that the maximum absorption is 57 dB/m at 1945 nm. These curves are derived by scaling the peak measured fiber absorption to the gain and absorption data reported in [14]. The validity of this scaling is confirmed by comparing the resulting gain and absorption curves to experimentally measured values [23] for the Ho-doped fiber under study. A first analysis indicates that pumping at or near 1940 nm might yield an optimum result because this is close to the wavelength for peak absorption. However, if we consider the additional effect of the gain curve, we can also hypothesize that pumping at 1940 nm where the gain is near its maximum value could lead to a reduction in the gain because of strong stimulated emission. This stimulated emission then reduces the population inversion created for the 2000–2100 nm signal band.
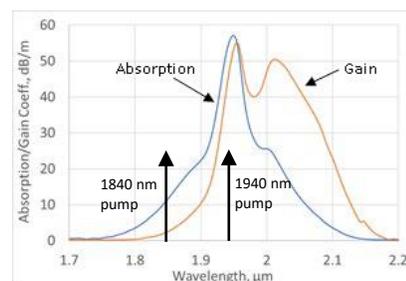
Fig. 1. Gain and absorption coefficients for HDF IXF-HDF-PM-8-125.

Based on our inferences for stimulated emission at the pump wavelength, we hypothesize that, for Ho-doped fibers, in-band pumping at wavelengths of 1820–1900 nm might be more efficient and effective than in-band pumping at wavelengths of 1940 nm and above. From Fig. 1 we see that the stimulated emission when pumping at 1820–1900 nm is expected to be far less that for a pump wavelength of 1940 nm. We note that our hypotheses are quite similar to behavior observed with in-band pumped Er-doped fiber amplifiers for the two pumping wavelengths of 1480 nm and 1529 nm and a signal band of 1530–1610 nm [21],[22].

With these considerations in mind, we start our quantitative analysis by considering the simple single stage HDFA shown in Fig. 2. Here signal input light at 2000–2100 nm passes though isolator I1 and signal/pump wavelength division multiplexer WDM1 and is coupled into F1, a PM Ho-doped fiber (iXblue IXF-HDF-PM-8-125). The signal output from F1 is coupled through isolator I2 to the signal output port. Internal input signal power P_s is measured at the input of F1, and internal signal output powers are measured at the output of F1. In this amplifier, P1 is a multiwatt 1720–2000 nm Tm-doped fiber laser which co-pumps F1 through WDM1. P1 can also be a semiconductor source or a solid-state laser source. Up to 2.5 W of 1720–2000 nm pump light is available to pump F1. Pump powers are measured at the input of F1. We note that Tm-doped fiber lasers can readily be engineered to produce multiwatt output powers over a wavelength band spanning 1800–1980 nm and more.
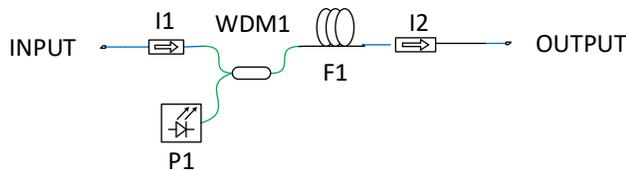
Fig. 2. Optical schematic of single stage PM HDFA.

To verify our hypotheses in a systematic way, we studied through simulations [10–12] the performance of a 3 m long Ho-doped amplifier in Fig. 2 as a function of pump wavelength. 3 m length was chosen based on previous optimization studies. Our simulations were carried out using proprietary software [10–12] using the Giles method [21,22] and fourth order Runge–Kutta algorithms, and incorporated a core diameter of 8 microns, an NA of 0.16, background losses of 200 dB/km for both pump and the signal wavelengths, and an ion pairing coefficient of 13.5%. This ion pairing coefficient is consistent with the experimental results in [23] and is typical of existing Ho-doped fibers in manufacture.

The results of our first simulation analysis are presented in Fig. 3, where we plot the saturated output power at a signal wavelength of 2051 nm for a pump power of 2470 mW and pump wavelengths ranging from 1720 nm to 2000 nm. Here we see that the signal output power reaches a maximum of 1033 mW at a pump wavelength of 1840 nm and maintains a high output value over the range of 1790–1930 nm. At 1940 nm pump wavelength, the output power is considerably reduced from the peak value to 425 mW. The numerical advantage of pumping at 1840–1860 nm relative to 1940 nm is therefore a factor of 2.43 or 3.9 dB in power. The peak optical-optical efficiency at 1840 nm is ε = 41.8%, and the efficiency

is reduced to 17.2% for 1940 nm pumping.
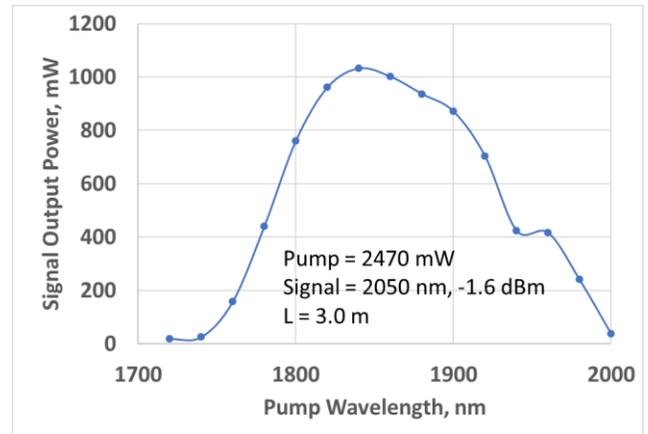
Fig. 3. Signal output power vs. pump wavelength for L = 3 m and λ$_s$ = 2050 nm.

Based on the results in Fig. 3, we then investigated the small signal gain and noise figure for the 3 m HDFA as a function of signal wavelength for the two selected pump wavelengths of 1860 nm and 1940 nm. Fig. 4 shows the simulated values of G and NF as a function of λ$_s$ for an input power of P$_s$ = -31.6 dBm. The advantage of pumping at 1860 nm is clear, where the peak gain at this pump wavelength is 54 dB in comparison to a peak gain of 45 dB for 1940 nm pumping. The simulated noise figures for the two pump
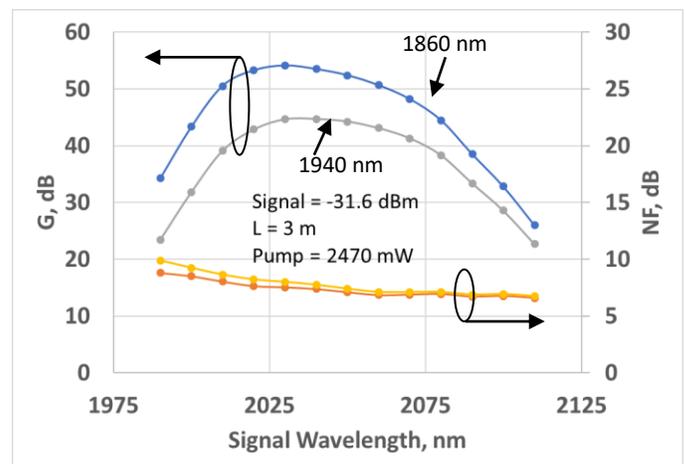
Fig. 4. Gain and noise figure vs. signal wavelength for L = 3 m and pump wavelengths of 1860 nm and 1940 nm.

wavelengths track one another closely with maximum noise figures of 10 dB at 1990 nm signal wavelength and minimum noise figures of 6.8 dB at 2110 nm.

We also simulated the saturated output power as a function of signal wavelength for the two selected pump wavelengths. Figure 5 plots output power vs. λ$_s$ from 1990 to 2110 nm. Here we see again the effectiveness of pumping at 1860 nm relative to 1940 nm, with an increase in peak power between the two pump wavelengths of 3.8 dB.

The signal output power with an 1860 nm pump is 1016 mW, corresponding to ε = 41.1%. At 1940 nm pump peak power is 426 mW corresponding to ε = 17.2%.
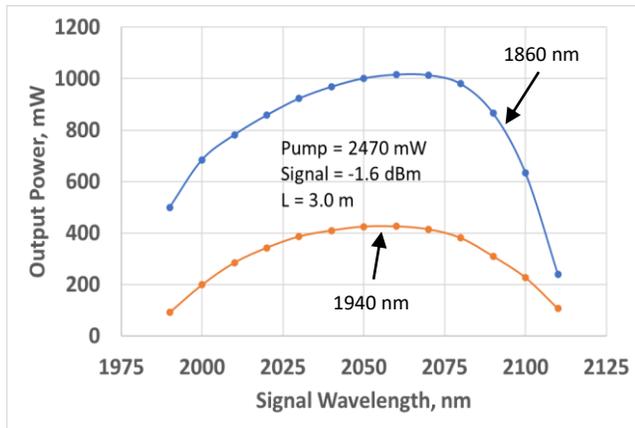
Fig. 5. Output power vs. signal wavelength for L = 3 m and pump wavelengths of 1860 nm and 1940 nm.

We have also studied through simulations the performance of the single stage amplifier design (Fig. 1) with a pump power limited to 1000 mW which is the level of pump that we can generate in a sub-miniature amplifier. Figure 6 shows the simulated output power for 1000 mW pump power as a function of fiber length for three pump wavelengths of 1860, 1940, and 2005 nm. The input signal power is -5 dBm at 2050 nm. Here we see that the optimum fiber length for this level of pump power is between 2.0 and 2.5 m for pump wavelengths of 1860 nm and 1940 nm. For a pump of 2005 nm, the amplifier is ineffective because of the low pump absorption and corresponding relatively high stimulated emission at this wavelength. Peak efficiencies are $\varepsilon = 26\%$ for 1860 nm pumping and $\varepsilon = 10.5\%$ for 1940 nm pumping.
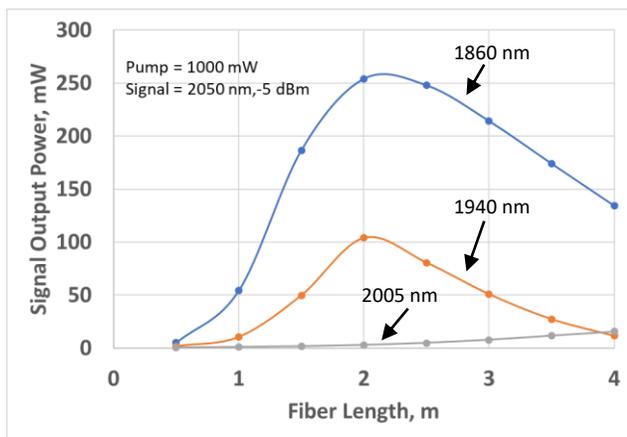
Fig. 6. Signal output power as a function of fiber length.

In Fig. 7 we plot simulated signal output power as a function of pump wavelength for F1 = 2.0 m, Ps = -5 dBm, and both co- and counter-propagating configurations. The graph shows that the optimum pump wavelength for this amplifier is 1860–1880 nm for co- and counter-pumping. For 1940 nm pump wavelength the output power decreases to a factor of 3.3 dB less than at the peak. Counter-pumping is slightly more efficient than co-pumping for this fiber length by a factor of 0.94 dB. The peak efficiency for counter-pumping is $\varepsilon = 31.5\%$.
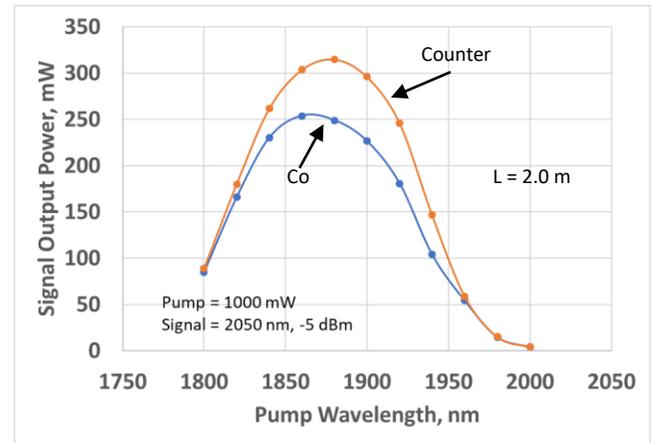
Fig. 7. Signal output power as a function of pump wavelength for co- and counter-propagating single stage HDFAs.

Figure 8 shows simulated output power vs. signal wavelength for L = 2.0 m and a pump of 1860 nm at 1000 mW. Here we see that counter-pumping is again slightly more efficient than co-pumping by about 0.82 dB, and the 3 dB output power bandwidth of the amplifier is 1995–2090 nm or 95 nm.
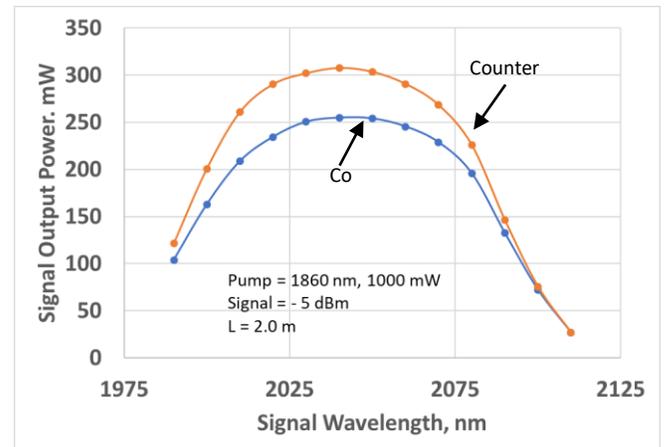
Fig. 8. Signal output power as a function of signal wavelength for co- and counter-propagating single stage HDFAs.

In Fig. 9 we plot simulated output power as a function of fiber length for a pump of 1860 nm at 1000 mW and a signal of 2050 nm at -5 dBm. From these data we observe that the optimum fiber lengths are between 2.0 and 2.5 meters for both the co-pumping and counter-pumping configurations. Once again counter-pumping yields output powers approximately 0.9 dB greater than co-pumping for this amplifier.
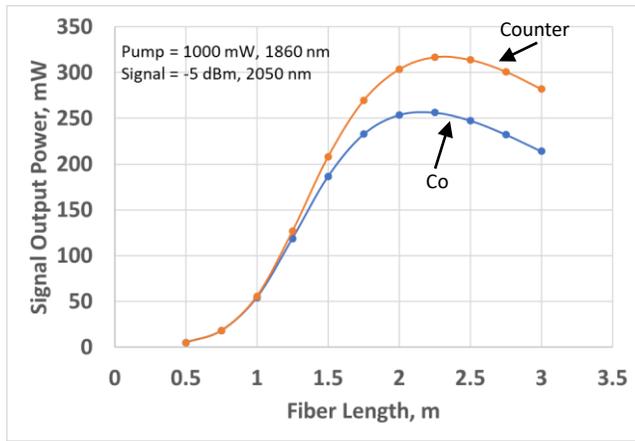
Fig. 9. Signal output power as a function of fiber length.

Figure 10 graphs simulated output power as a function of pump power for a signal of 2050 nm and -5 dBm, L = 2.0 m, and two representative pump wavelengths of 1860 nm and 1940 nm. We see from these results that 1860 nm pumping is again much more efficient than 1940 nm pumping for this amplifier, and that counter-pumping yields slightly more efficient operation than co-pumping. The slope efficiency for 1860 nm in the counter-pumping configuration is the high value of η = 56.6%. We note that the 1860 nm pumped amplifiers reach transparency at lower pump powers than the 1940 nm pumped amplifiers.
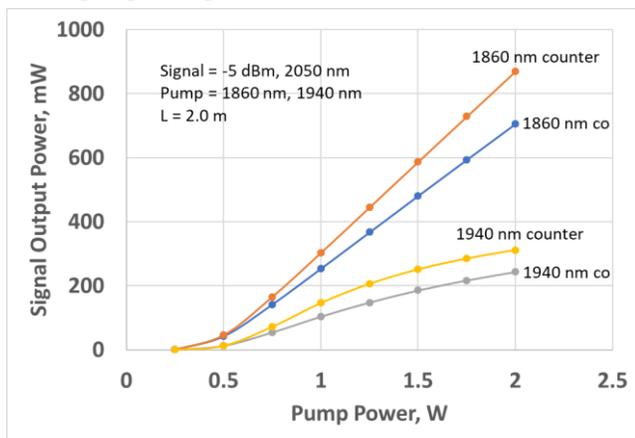
Fig. 10. Signal output power vs. pump power for co- and counter propagating HDFAs.

In summary, for all the configurations studied through simulations, we find that 1860 nm pumping is far more efficient than 1940 nm pumping, verifying our hypotheses based on the gain and absorption curves of Fig. 1.

III. COMPARISON OF SIMULATION WITH EXPERIMENT AND NEW DESIGN DIRECTIONS

To compare the results of our simulations with data, we first turn to an experimental measurement of the output power from the PM Ho-doped fiber with 1860 nm pumping. The single stage experimental setup for this measurement is shown in Fig. 11, with the following parameters: Pump power = 2.0 W at 1860 nm, signal input = 0.8 dBm at 2092 nm, and F1 = 3.0 m. The amplifier is counter-pumped instead of co-

pumped as in Fig. 1.
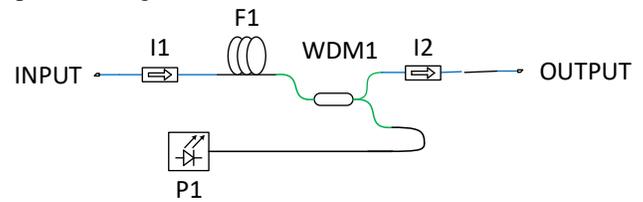
Fig. 11. Counter-pumped single stage PM HDFA.

The experimentally measured output power from the amplifier in Fig. 11 under these conditions is found to be 840 mW ± 15 mW, corresponding to a power conversion efficiency of 42%.

The simulated output power for this configuration is found to be 907 mW, which is 0.33 dB or 8% greater than the measured output power. This indicates excellent agreement between simulation and experiment for 1860 nm pumping.

We next study the variation in 2092 nm signal output power for this amplifier as a function of 1860 nm pump power. Fig. 12 plots the measured (points) and simulated (solid line) signal output power at 2092 nm as a function of pump power at 1860 nm with pump powers ranging from 0.26 W to 2.32 W. We see that the agreement between experiment and simulation is quite good, with typical variations between data and simulations of 0.5 dB or less. The optical-optical conversion efficiency slope for the simulated amplifier output is η = 37.3%.
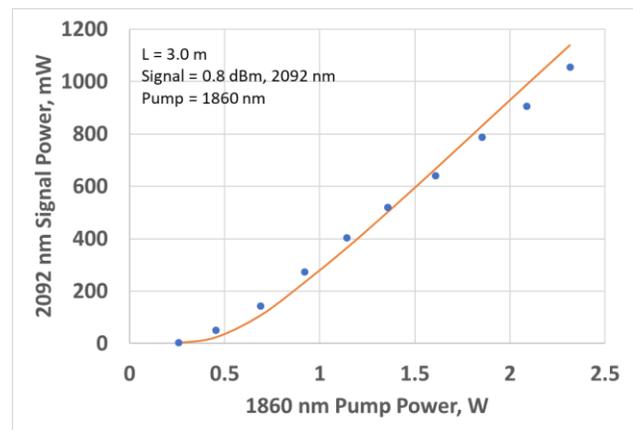
Fig. 12. Signal output power vs. pump power for counter-pumped single stage PM HDFA

Figure 13 gives a comparison of simulation and experiment for the optical signal-to-noise ratio (OSNR) for the amplifier signal at 2092 nm as a function of pump power. Here the experimental data are points and the simulation is a solid line. The typical simulated spectrum for a signal wavelength of 2092 nm and a pump power of 2.32 W is shown in Fig. 14. Here the gain peak is at 1940 nm and the 10 dB bandwidth is about 90 nm. We will address this spectral behavior more fully in a future publication. As the plot in Fig. 13 indicates, the simulations and the experimental data agree well over the measured pump range of 0.26–2.09 W at 1860 nm.
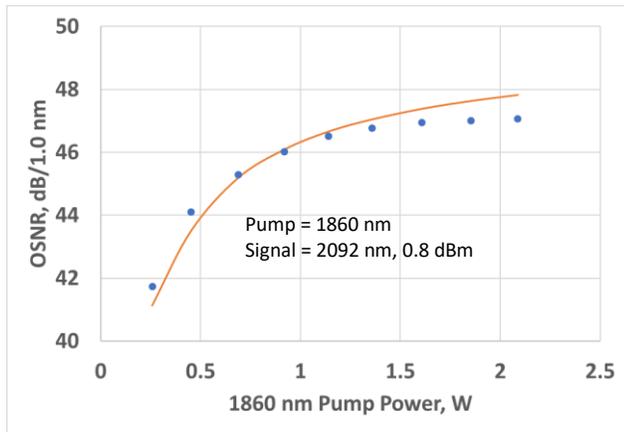
Fig. 13. Experimental and simulated OSNR for counter-propagating PM HDFA.
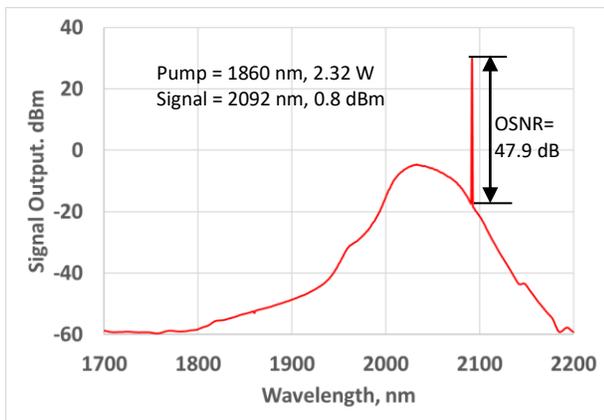
Fig. 14. Simulated spectrum for counter-propagating PM HDFA.

In Fig. 15 we graph the simulated vs. experimental values of output signal power vs. input signal power for an 1860 nm pump power of 1.26 W. The plot demonstrates that agreement between simulation and experiment is relatively good over the full range of input powers studied. The differences for lower input powers are under study. We will address this subject more fully in a future publication.
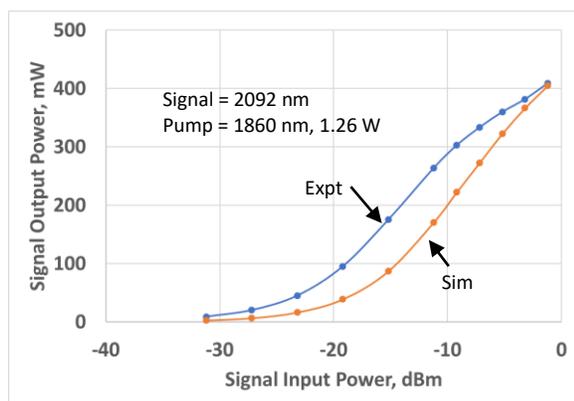
Fig. 15. Output signal power vs. input signal power at 2092 nm for counter-propagating HDFA.

Next we compare the performance of a co-pumped 3 m HDFA with 1940 nm pumping and an input signal of 0 dBm at 2050 nm. Figure 16 shows the experimentally measured output power (blue points) and the simulated output powers (orange line) for this amplifier. We see that the agreement between experiment and simulation is excellent for this amplifier with less than 0.2 dB differences between the simulations and the data. This directly confirms our hypotheses about 1860 nm vs. 1940 nm pumping.
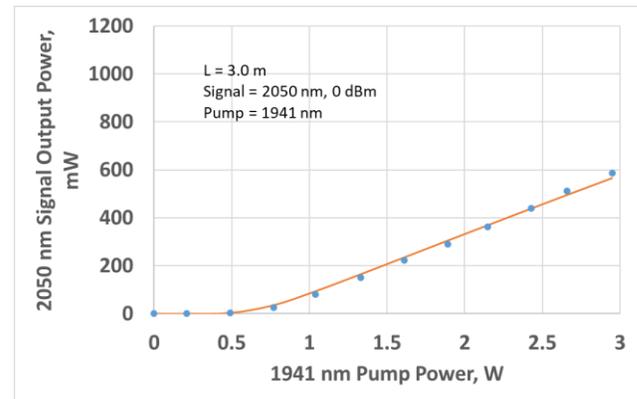
Figure 16. Comparison of experiment and simulation for a co-pumped HDFA pumped at 1940 nm.

Finally, to verify simulations at 1940 nm, we consider a two-stage PM HDFA optimized for 1940 nm pumping. The optical architecture of this two stage amplifier [12] is shown in Fig. 17. Here the pump source at 1940 nm is split between the two co-pumped amplifier stages with 30% power to F1 and 70% power to F2. The total amount of pump power available is 4.6 W. The fiber lengths are F1 = 3.0 m and F2 = 2.0 m. The signal input power is 0 dBm at 2051 nm, and the signal insertion loss of the interstage isolator + WDM is 1.6 dB.
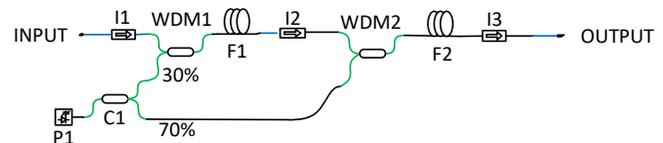
Fig. 17. Two-stage PM HDFA pumped at 1940 nm.

Under these conditions, we found that the experimentally measured output power was +32.57 dBm or 1807 mW ± 25 mW for a signal wavelength of 2051 nm and an input power of -1.6 dBm.

Simulations of this amplifier configuration yielded a signal output power of 1681 mW, which is 7% or 0.32 dB lower than the measured data. Once again this indicates quite good agreement between simulation and experiment.

Taken together, we find that simulations and experimental results agree quote well for the wide range of parameters and architectures covered by our studies.

Moving forward from the 1940 nm two-stage amplifier architecture, we now investigate the optimum configuration for a two-stage amplifier pumped at 1860 nm. After multiparameter optimization studies, we find that the best performance is achieved with a split ratio of 15% pump power to F1, 85% pump power to F2, and fiber lengths of F1 = 1.88 m and F2 = 1.75 m. Figure 18 compares the simulated output power vs. pump power performance of the 1860 nm optimized two stage amplifier with the 1940 nm two stage

amplifier. We see that the optimized 1860 nm amplifier considerably outperforms the 1940 nm amplifier, with a difference in maximum output powers of +1.63 dB or 46%. The optical-to-optical conversion efficiency ε and slope η for 1860 nm are ε = 53.2% and η = 63.5%. For 1940 nm, ε = 36.5% and η = 48.0%. This clearly demonstrates, once again, the significant advantages of 1860 nm pumping.
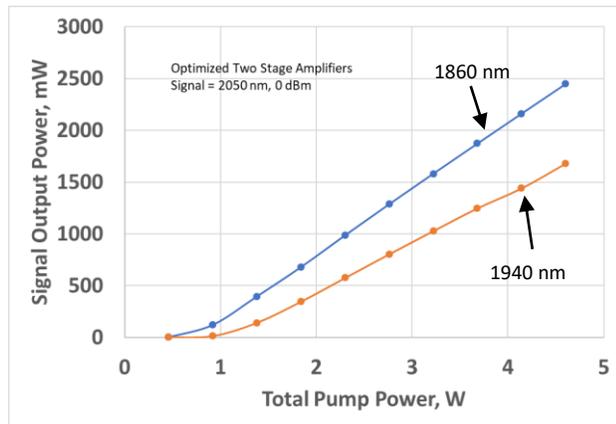
Fig. 18. Comparison of simulated output power vs. pump power performance of optimized 1860 nm and 1940 nm pumped two stage amplifiers.

IV. DISCUSSION

To our knowledge, our presentation of 1860 nm in-band pumping for a Ho-doped fiber amplifier is the first discussion of a noteworthy in-band alternative pump wavelength for this amplifier system. Previous published work has used pump wavelengths almost exclusively at or near 1940 nm [8]–[20], [29]. A high wavelength pump near 2000 nm was investigated in [15], [19] and found to yield suboptimum results.

The results presented here are valid for HDFAs with medium slope efficiencies in the range of 64% (see Fig. 18). While higher slope efficiencies of 61–85% have been experimentally observed in prototype solution doped and nano-particle doped HDFAs [24], and 87% in a laser in [17], we note that our experimental and simulation results are valid for a quite wide range of commercially available Ho-doped fibers.

We observe that in-band pumping at or near 1860 nm has several additional significant advantages, in addition to the ones already mentioned, over the previous technical standard of 1940 nm.

First, the wavelength tolerance for the pump is much larger in the 1860 nm band than it is in the 1940 nm region, as illustrated by Fig. 2. The saturated output power is largely insensitive to pump wavelength from 1820–1880 nm, where in contrast for 1940 nm the output power varies significantly with small changes in pump wavelength. Also, the fiber reaches transparency at lower powers for 1860 nm pumping than for 1940 nm pumping.

Second, the lower wavelength of 1860 nm yields better crosstalk between pump and signal wavelengths because of the larger separation compared to 1940 nm. It is easier to construct WDMs with very low pump to signal crosstalk at 1860 nm than it is at 1940 nm.

Third, this larger wavelength separation also contributes to a lower noise figure because of greater population inversion in the fiber for 1860 nm pumping than for 1940 nm pumping.

While much work has been carried out on the pumping of single clad Ho-doped fiber amplifiers at or near 1120 nm [25]–[28], the reported slope efficiencies for this pump wavelength are all suboptimum and in the range of 20–30%. We also observe that it is quite difficult to fabricate a fiber that is robustly single mode for both the pump wavelength of 1120 nm and the signal wavelength band of 2000–2120 nm. For these reasons we have chosen to concentrate on the performance of in-band pumped HDFAs.

Our comparison of experiments and calculations show that, for 1860 nm pumping and a single stage counter-pumped medium slope efficiency HDFA, there is good agreement between data and simulations for output power vs. pump power, OSNR vs. pump power, and the output spectra vs. input signal power. Typical agreements between experiment and simulation are on the order of ± 0.5 dB or less. For 1940 nm pumping of a single stage and a two stage co-pumped HDFA, we found equally good agreement between simulations and data for signal output power values. The good agreement fully validates our simulation approach to determining the performance of single stage and multi-stage HDFAs.

Finally, we note that strong similarities exist between the Ho-doped fiber amplifier pumped at 1860/1940 nm and the Er-doped fiber amplifier pumped at 1480/1531 nm [21], [22]. For both of these systems, in- band pumping at the peak of the absorption curve results in significantly degraded performance relative to pumping at a judiciously selected lower wavelength. This confirms our initial hypotheses based on observation of the gain and absorption coefficients for the PM Ho-doped fiber.

V. SUMMARY AND CONCLUSIONS

We have presented a novel and innovative in-band pumping wavelength of ~1860 nm for medium slope efficiency Ho-doped fiber amplifiers operating in the 2000–2100 nm signal region. The clear performance advantages of this new pumping wavelength are verified both through simulations and experiment. Compared to the previous industry and research standard pumping wavelength of 1940 nm, we have demonstrated that 1860 nm pumping can yield significantly higher output powers, small signal gains, and power conversion efficiencies in current amplifier architectures. In the case of single stage designs, the advantages in output power are typically 3–4 dB, and the advantages in small signal gain are found to be as great as 8–10 dB. The application of our findings to other single- and double-clad fiber amplifiers and to fiber lasers with lower background losses and lower ion pairing coefficients, and in particular for higher slope efficiency HDFAs, will be studied in a future publication.

Taken together, our results clearly demonstrate the strong advantages of this novel ~1860 nm pumping approach for medium slope efficiency HDFAs. We anticipate immediate applications in the design and manufacture of single and multi-stage HDFAs and ASE sources for LIDAR, lightwave communications systems, coherent lightwave systems, and spectral sensing applications.

VI. References

[1] G. D. Spiers et al., "Atmospheric CO_2 measurements with a 2 µm airborne laser absorption spectrometer employing coherent detection," Applied Optics 50, 2098-2111 (2011).

[2] J. Caron and Y. Durand, "Operating wavelengths optimization for a spaceborne lidar measuring atmospheric CO2," Applied Optics 48, 5413–5422 (2009).

[3] J. B. Abshire, H. Riris, G. R. Allan, C. J. Weaver, J. Mao, X. Sun, W. E. Hasselbrack, and A. Yu, A. Amediek, Y. Choi, and E. V. Browell, "A lidar approach to measure CO2 concentrations from space for the ASCENDS mission," Proc. SPIE 7832, 783201 (2010).

[4] M. U. Sadiq et al., "40 Gb/s WDM Transmission Over 1.15-km HC-PBGF Using an InP-Based Mach-Zehnder Modulator at 2 µm," J. Lightwave Technology 34, 1706-1711 (2016).

[5] H. Zhang et al., "Dense WDM Transmission at 2 µm Enabled by an Arrayed Waveguide Grating," Optics Letters 40, 3308-3311 (2015).

[6] H. Zhang et al., "100 Gbit/s WDM Transmission at 2 µm: Transmission Studies in Both Low-loss Hollow Core Photonic Bandgap Fiber and Solid Core Fiber," Optics Express 23, 4946-4951 (2015).

[7] H. Zhang et al., "81 Gb/s WDM Transmission at 2 µm over 1.15 km of Low-Loss Hollow Core Photonics Bandgap Fiber," in Proc. ECOC 2014, Cannes, France, paper P.5.20.

[8] R. E. Tench, C. Romano, and J.-M. Delavaux, "A 25 W 2 µm Broadband Polarization-Maintaining Hybrid Ho- and Tm-Doped Fiber Amplifier," Applied Optics 58, 4170-4175 (2019).

[9] Robert E. Tench, Clement Romano, and J.-M. Delavaux, "Studies of the Optical Bandwidth of a 25 W 2 µm Band PM Hybrid Ho-/Tm-Doped Fiber Amplifier", in Proc. SPIE 11000, Fiber Optic Sensors and Applications XVI, Defense and Commercial Sensing, Baltimore, MD, Paper 11000-8 (April 2019).

[10] R. E. Tench, C. Romano, J-M. Delavaux, T. Robin, B. Cadier, and A. Laurent, "Broadband High Gain Polarization-Maintaining Holmium-doped Fiber Amplifiers," in Proc. ECOC 2018, Rome, Italy, September 2018, Paper Mo3E.3.

[11] Robert E. Tench, Clement Romano, Glen M. Williams, Jean-Marc Delavaux, Thierry Robin, Benoit Cadier, and Arnaud Laurent, "Two-Stage Performance of Polarization-Maintaining Holmium-Doped Fiber Amplifiers," IEEE Journal of Lightwave Technology 37, 1434—1439 (2019).

[12] Robert E. Tench, Clement Romano, and Jean-Marc Delavaux, "Shared Pump Two-Stage Polarization-Maintaining Holmium-Doped Fiber Amplifier," IEEE Photonics Technology Letters 31, 357—360 (2019).

[13] R. E. Tench et al., "In-Depth Studies of the Spectral Bandwidth of a 25 W 2 µm Band PM Hybrid Ho- and Tm-Doped Fiber Amplifier", J. Lightwave Technol., vol 38, pp. 2456—2463 (2020).

[14] A. Hemming, N. Simakov, A. Davidson. M. Oermann, L. Corena, D. Stepanov, N. Carmody, J. Haub, R. Swain, and A. Carter, "Development of high-power Holmium-doped fibre amplifiers," Proc. SPIE 8961, Fiber Lasers XI: Technology, Systems and Applications, 89611A (7 March 2014).

[15] N. Simakov, Z. Li, Y. Jung, J. M. O. Daniel, P. Barua, P. C. Shardlow, S. Liang, J. K. Sahu, A. Hemming, W. A. Clarkson, S-U. Alam, and D. J. Richardson, "High Gain Holmium-doped Fibre Amplifiers," Optics Express 24, 13946-13956 (2016).

[16] N. Simakov, Z. Li, U. Alam, P. C. Shardlow, J. M. O. Daniel, D. Jain, J. K. Sahu, A. Hemming, W.A. Clarkson, and D. Richardson, "Holmium Doped Fiber Amplifier for Optical Communications at 2.05

2.13 µm," in Proc. OFC 2015, Paper Tu2C.6.

[17] A. Hemming, N. Simakov, M. Oermann, A. Carter, and J. Haub, "Record Efficiency of a Holmium-doped Silica Fibre Laser," in Proc. CLEO 2016, Paper SM3Q.5.

[18] N. Simakov, A. Hemming, W. A. Clarkson, J. Haub, and A. Carter, "A cladding-pumped, tunable holmium doped fiber laser", Optics Express 21, 28415—28422 (2013).

[19] N. Simakov, "Development of components and fibres for the power scaling of pulsed holmium-doped fibre sources," Ph.D. thesis (University of Southampton, 2017).

[20] J. Wang, D. I. Yeom, N. Simakov, A. Hemming, A. Carter, S. B. Lee, and K. Lee, "Numerical modeling of in-band pumped Ho-doped silica fiber lasers," J. Lightwave Technol. 36, 5863–5880 (2018).

[21] C. R. Giles, C. A. Burrus, D. DiGiovanni, N. K. Dutta, and G. Raybon, "Characterization of erbium-doped fibers and application to modeling 980-nm and 1480-nm pumped amplifiers," IEEE Photon. Technol. Lett. 3, 363–365 (1991).

[22] E. Desurvire et al., "Erbium-Doped Fiber Amplifiers: Device and System Developments", Wiley, 2003.

[23] J. LeGouet, F. Gustave, P. Bourdon, T. Robin, B. Cadier, and A. Laurent, "Realization and simulation of high-power holmium doped fiber lasers for long-range transmission," Optics Express 28, 22307 (2020).

[24] Colin C. Baker, E. Joseph Friebele, Ashley A. Burdett, L. Brandon Shaw, Steven R. Bowman, Woohong Kim, Jasbinder S. Sanghera, John M. Ballato, Courtney Kucera, Amber Vargas, Alexander V. Hemming, Nikita Simikov, and John Haub, "Recent advances in holmium doped fibers for high-energy lasers," Proceedings Volume 10637, Laser Technology for Defense and Security XIV; 1063704 (2018).

[25] S O Antipov and A S Kurkov, "A holmium-doped fiber amplifier at 2.1 µm," Laser Phys. Lett. 10, 125106 (2013).

[26] S A Filatova, V A Kamynin, V B Tsvetkov, O I Medvedkov and A S Kurkov, "Gain spectrum of the Ho-doped fiber amplifier," Laser Phys. Lett. 12 095105 (2015).

[27] V.A. Kamynin, S.O. Antipov, A.V. Baranikov and A.S. Kurkov, "Holmium-doped fibre amplifier operating at 2.1 um," Quantum Electron. 44, 161 (2014).

[28] V. A. Kamynin, S. A. Filatova, I. V. Zhluktova and V. B. Tsvetkov, "Holmium doped fiber amplifier in the spectral region 2–2.15 um," 2016 International Conference Laser Optics (LO), St. Petersburg, Russia, 2016, pp. S1-17.

[29] R. E. Tench et al., "3.5 W Broadband PM Hybrid Amplifier at 2051 nm With Holmium- and Thulium-Doped Single-Clad Fibers," in Journal of Lightwave Technology, vol. 39, no. 5, pp. 1471-1476, (2021), DOI: 10.1109/JLT.2020.3034477.